

SCIENTIFIC REPORTS



OPEN

No protection of permafrost due to desertification on the Qinghai–Tibet Plateau

Qingbai Wu, Wenbing Yu & Huijun Jin

Desertification of tundra regions may form an escalating cycle with permafrost degradation where more permafrost thaw leads to continued desertification. This traditional viewpoint has been challenged in recent reports that state desertification protects the underlying permafrost. However, our measurements of soil temperature from nine sites in the Honglianghe River Basin, interior Qinghai–Tibet Plateau, show that desertification can degrade permafrost. If one compares the permafrost temperatures at sites with thin sand covers (e.g. site Yu-7, permafrost temperature of -0.64°C ; site Yu-6, permafrost temperature of -1.15°C) with that of site Xie-1 (-0.65°C , with a 120-cm-thick sand cover), the permafrost temperature is not significantly different. It is clear that a thick sand cover does not influence the underlying permafrost temperature. Our observations support traditional geocryological knowledge which states that, under most circumstances, desertification does not protect, but rather degrades, permafrost.

Permafrost is defined as ground that remains continuously at or below 0°C for at least two consecutive years¹. Permafrost is a product of long-term energy exchange between the ground surface and atmosphere and is therefore a condition of ground climate². The difference in the macro-scale distribution of permafrost is controlled by the climate³; however, the difference in the local conditions, such as the topography, vegetation, snow cover, soil and geological conditions, can significantly modify the thermal impacts of the climate^{4–6} and result in local-scale anomalies in permafrost distribution³.

One of the local-scale factors influencing permafrost distribution is dominantly surface cover, e.g. vegetation, snow cover, and water⁷. Many studies have presented the thermal effects of local-scale surface cover on the active layer processes, e.g., the hydrothermal regimes and ground freezing–thawing in the active layer, active layer thickness, and thermal states of permafrost^{3, 8–11}. However, little focus has been placed on the hydrothermal impacts of desertification (sand layer or dune formation over the frozen ground) on the thermal regimes of soils in the active layer and the underlying permafrost.

Permafrost underlies approximately 70% of the land area of the Qinghai–Tibet Plateau (QTP), the highest and most extensive plateau permafrost on Earth^{12–14}. Observational evidence demonstrates that warming, thawing and degrading of the plateau permafrost has occurred during the past few decades^{11, 13, 15–19}. The effect of permafrost degradation in the Qinghai–Tibet Plateau dries the ground surfaces because the active layer usually thickens, the permafrost table lowers and vegetation becomes more fragmented and sparse. The result is an increase in wind action, enhanced deflation and Aeolian deposition, and increased potential risk of desertification^{16, 20–22}.

Since the 1960s, grassland deterioration and desertification have occurred in some parts of the QTP^{23–25} and Northeast China²⁵. However, a number of recent studies^{26–28} have concluded that a surface cover of wind-blown sand actually protects the underlying permafrost on the QTP. These studies are based on short-term data from only one field site and are in conflict with traditional geocryological knowledge^{20, 21, 29, 30}. Accordingly, we review the relationships between land desertification and permafrost degradation at the Qinghai–Tibet Plateau and discuss the spatial distribution of permafrost on the QTP. We assess the effect of a surface sand layer on ground heat transfer via modeling informed by field and laboratory measurements.

Data and Method

Nine sites around the Xie *et al.*²⁸ study site were established in 2012 for ground temperature monitoring in the Honglianghe River basin (Fig. 1; Table 1). The geographical information, sand cover, permafrost temperature and

State Key Laboratory of Frozen Soils Engineering, Northwest Institute of Eco-Environment and Resource, Chinese Academy of Science, Lanzhou, 730000, China. Correspondence and requests for materials should be addressed to Q.W. (email: qbwu@lzb.ac.cn)

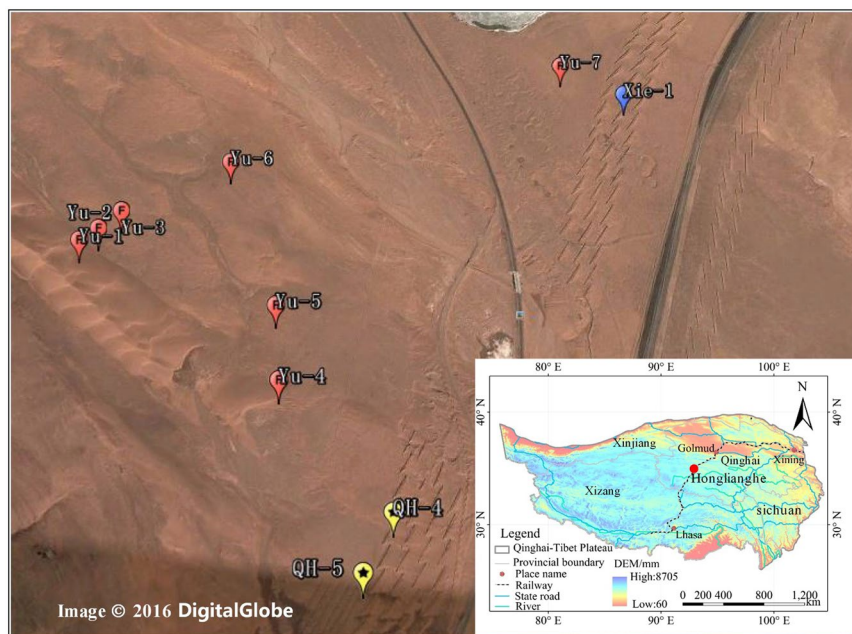


Figure 1. Map of observation sites at the Honglianghe River Basin along the Qinghai-Tibet Highway of the interior Qinghai-Tibet Plateau (the map was edited and generated using Google Earth, Image© 2016 DigitalGlobe; the small map was edited and generated using ArcGIS 8.0, which is American GIS Software (<http://www.esrichina.com.cn/softwareproduct/ArcGIS/>); Qingbai Wu created this map).

Sites	Longitude (°E)	Latitude (°N)	Surface condition	MAGT (°C)	ALT (m)	SFT (m)	Observation methods for GT
Yu-1	35.0490	93.0069	Sand cover, 3.3 m in thickness	1.03		—	Manual
Yu-2	35.0495	93.0071	Desert with sparse vegetation	0.58		—	
Yu-3	35.0498	93.0076	Desert with sparse vegetation	0.89		—	
Yu-4	35.0466	93.0119	Sand cover, 3.0 m in thickness	0.84		4.0	Automatically collected by data logger CR3000
Yu-5	35.0481	93.0115	Desert with sparse vegetation	0.92		3.8	
Yu-6	35.0513	93.0097	Desert with sparse vegetation	-1.15	2.0		Manual
Yu-7	35.0542	93.0147	Desert with sparse vegetation	-0.64	3.5		
QH-4	35.0444	93.0147	Sand cover, 30 cm in thickness	0.30		4.5	Automatically collected by data logger CR3000
QH-5	35.0434	93.0143	Sand cover, 115 cm in thickness	-0.74	3.2		

Table 1. Geographic information, surface conditions, mean annual ground temperature (MAGT), active layer thickness (ALT), seasonally frozen ground thickness (SFT) and observation methods for ground temperatures (GT) at the nine study sites.

active layer thickness are shown in Table 1. These sites had different thicknesses of sand cover. One site (site Yu-7) is located near to the soil temperature monitoring site discussed by Xie *et al.* (site Xie-1)²⁸ (see Fig. 1).

In this area of the QTP, climate data from Wudaoliang (from 2010 to 2014, 15 km from the study sites) indicates mean annual air temperature varies from -3.8°C (2010) to -4.6°C (2012) with an average of -4.2°C .

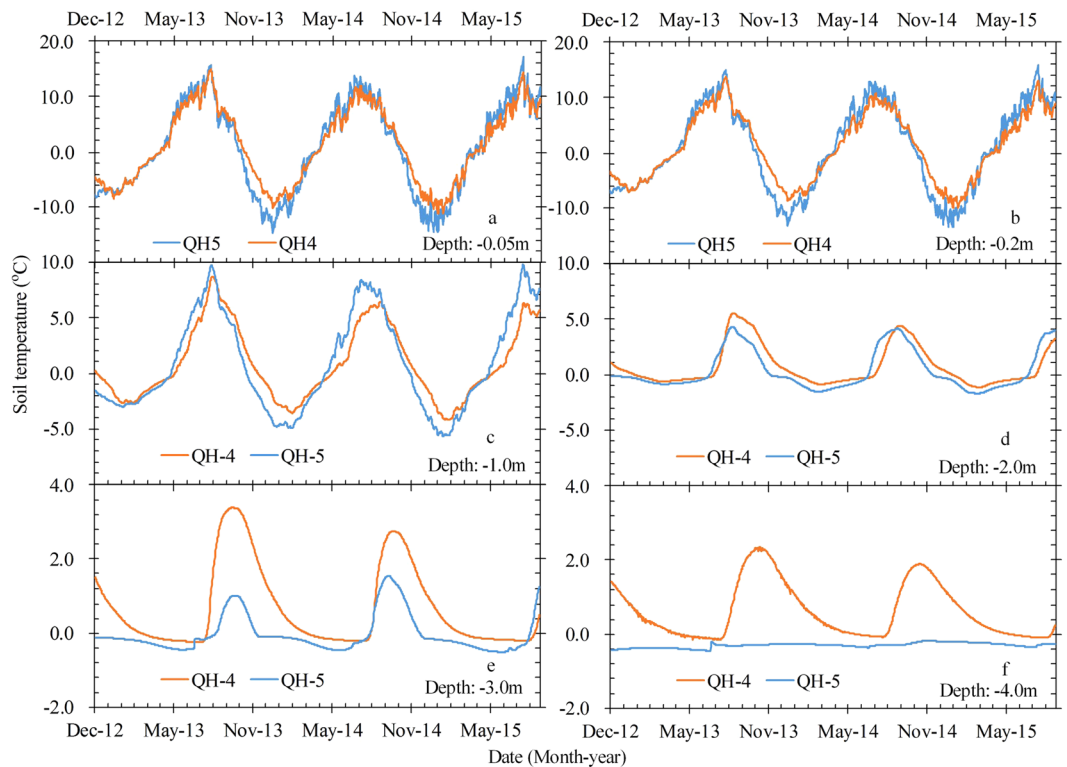


Figure 2. Variations in soil temperatures at depths of 0.05 m (a), 0.2 m (b), 1.0 m (c), 2.0 m (d), 3.0 m (e), and 4.0 m (f) at QH-4 (30 cm sand layer) and QH-5 (115 cm sand layer) in the Honglianghe River Basin during the observation period from 1 December 2012 to 28 August 2015.

Annual precipitation varies from 273 mm (2013) to 425 mm (2012) with an average of 369 mm. Mean annual air temperatures in the summer months (JJA) vary from 4.13 to 7.2 °C, with an average of 5.7 °C. In the winter months (DJF) mean annual air temperatures vary from −13.47 to −14.67 °C, with an average of −14.0 °C.

Soil temperature were measured at depths of 0.1 to 18.0 m using thermistor strings at depth increments of 0.5 m that were assembled by the State Key Laboratory of Frozen Soils Engineering (SKLFSE) at Lanzhou, China. The temperature accuracy of these sensors is ± 0.05 °C. For all sites, the *in-situ* measurements were conducted in two ways: (i) some were recorded manually on the 5th and 20th days of each month, (ii) others were collected daily by data loggers (CR3000, Campbell Scientific Inc., USA). Three sites were underlain by permafrost (Yu-6, Yu-7, QH-5), the others experience deep seasonal frost.

Results

Subsurface soil temperatures. Figure 2 shows variations in soil temperatures at depths of 0.05 m to 4.0 m under (i) a 0.3-m-thick sand cover at site QH-4 (deep seasonal frost) and (ii) a 1.15-m-thick sand cover at site QH-5 (permafrost). Ground temperatures at site QH-4 are lower than those at site QH-5 during the summer months but higher during the winter months in the near-surface (0.05 m to 2.0 m depth) (Fig. 2a–d). However, at depths of 3 to 4 m, temperatures at QH-5 are colder than those at QH-4 (Fig. 2e,f) and the MAGT at site QH-5 is lower than that at site QH-4 (Fig. 3). It is clear that the mean daily and mean annual ground temperatures change with the thickness of the sand cover; as the thickness of the sand cover increases, the soil temperature decreases. This pattern is similar to the pattern observed by Xie *et al.*²⁸ but it does not explain how the sand layer (or sand veneer) protects the underlying permafrost from thermal change. In other words, conclusions cannot be drawn from ground temperatures observed at just one borehole.

Thermal regime of permafrost under sand cover. Figure 4 shows the thermal regimes of ground under different sand covers that were measured at observation sites close to the observation site of Xie *et al.*²⁸ in the Hongliang River Basin. The data demonstrates that seasonal frozen ground can be found under a 3.0-m-thick sand cover at site Yu-4 and also under a 0.3-m-thick sand cover at site QH-4. At the same time, the permafrost temperature under a sand dune with sparse vegetation at a depth of 14 m is −1.15 °C (site Yu-6) yet it is −0.74 °C under a 1.15-m-thick sand cover at site QH-5. When one compares the permafrost temperature at dune-free sites (site Yu-7, −0.64 °C and site Yu-6, −1.15 °C) with that at site Xie-1 (with a 120-cm-thick sand cover), the permafrost temperature at site Xie-1 is −0.65 °C²⁸, clear, therefore, that a thick sand cover does not significantly influence the underlying permafrost temperature.

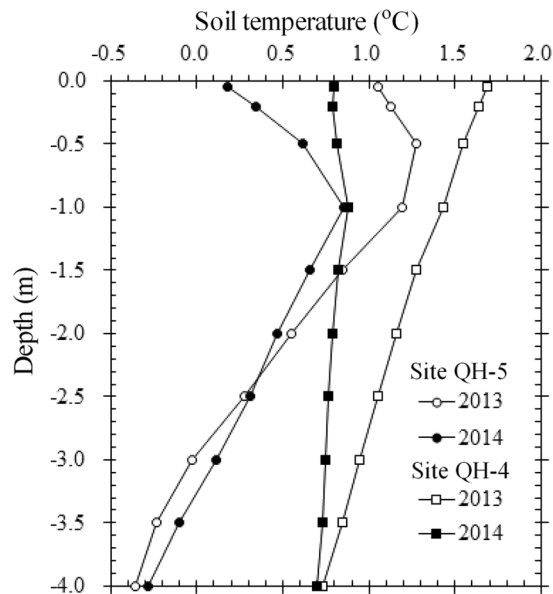


Figure 3. Mean annual soil temperature in 2013 and 2014 at 0.1 to 4.0 m depths at sites QH-4 (30 cm sand layer) and QH-5 (115 cm sand layer) in the Honglianghe River Basin.

Permafrost temperature. The permafrost at the nine sites monitored by the authors shows a strong spatial heterogeneity. Regarding MAGT, permafrost has strong spatial heterogeneity caused by various thicknesses of the sand cover in the Honglianghe River area. For example, no permafrost is found at sites Yu-1 to Yu-5 (desert with sparse vegetation) in spite of variations in sand-cover thickness. Permafrost also occurs at sites Yu-6 and Yu-7 (deserts with sparse vegetation) and at site QH-5 (with 115-cm-thick sand cover). The mean annual ground temperature (MAGT) at two non-permafrost sites ranges from $+0.3^{\circ}\text{C}$ at the YU-6 site to -1.15°C at the QH-4 site. The average is -0.6°C . The MAGTs from three Xie *et al.*²⁸ sites are estimated from Fig. 1 to range from approximately -0.5°C to -0.7°C .

If sand cover, or desertification, has a role in protecting the underlying permafrost, it should be observed widely across the Honglianghe River Basin. However, our observations show permafrost does not exist at sites with either a sand cover of 3.0 to 3.3 m in thickness or with barren surfaces possessing very sparse vegetation. On the other hand, permafrost occurs at sites with possess either a thin sand cover (30 cm to 115 cm in thickness) or are barren and with sparse vegetation or barren (Table 1). Obviously, spatial difference alone cannot verify whether sand cover, or desertification, protects the underlying permafrost.

Discussion

Relationships between desertification and permafrost. Permafrost plays a fundamental role in the alpine ecosystems of the Qinghai-Tibet Plateau^{31,32}. If warming is not accompanied by increased precipitation, permafrost degradation causes a lowering of the water table, vegetation degradation and desertification^{13,21,29,30,32,33}. A positive feedback mechanism is also present: the decreased vegetative coverage increases surface energy fluxes that can lead to ground warming and further desertification³².

Interestingly, if desertification can protect underlying permafrost, as claimed by Xie *et al.*^{26–28}, it follows that Late Pleistocene permafrost should be well-preserved in the cold deserts of western China. The maximum southern limit of latitudinal permafrost in China during the Last Glacial Maximum (LGM) was approximately $5\text{--}10^{\circ}$ latitude beyond the present-day southern permafrost limit at $46^{\circ}\text{--}47^{\circ}\text{N}$ ^{34,35}. However, no sand-wedge casts or ice-wedge pseudomorphs or other periglacial phenomena indicative of the occurrence of either past or present permafrost have been found on or around sand dunes in the desert regions of western China³⁴; however, they have been identified in oases such as wetlands, river valleys and terraces in those desert regions. Actually, in many high plateau and alpine regions, permafrost is generally absent in deserts, although talik is extensively identified under deserts or desertified lands with active sand dunes.

Local heterogeneity of permafrost occurrence. The permafrost distribution across the Qinghai-Tibet Plateau has a strong spatial heterogeneity that is influenced by local factors such as vegetation, soil texture and stratigraphy. Illustrations of this heterogeneity include (i) the distribution of permafrost in the Liangdahe River Basin along the QTH³⁶, (ii) the distribution of permafrost along the eastern side of the QTH where permafrost occurs extensively under paludal alpine meadows with a mean annual ground temperature (MAGT) of approximately -1.2°C and a permafrost thickness of more than 60 m³⁷, no permafrost can be found along the western side of the highway due to human-induced degradation of the alpine meadows, and (iii) the distribution of permafrost in the Beiluhe River Basin along the QTR where the MAGT ranges from -0.4°C to -1.8°C across an area of 5 km^2 ^{2,38} and where, at the Fenghuoshan Mountain Pass, the MAGT on the north and south slopes differs by approximately 2°C , and at the Kunlunshan Mountain Pass by approximately 1.5°C ³⁹. Thus, permafrost

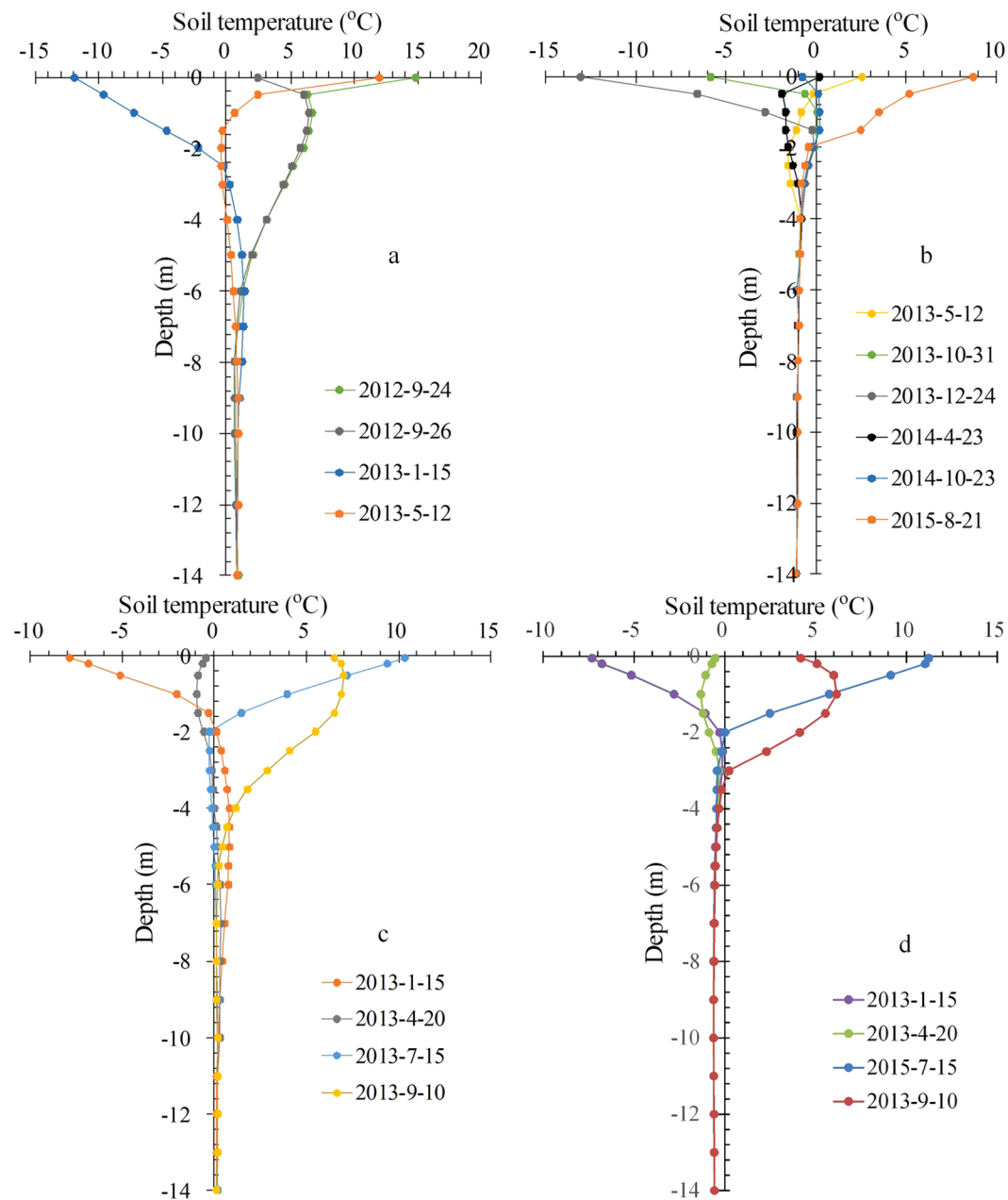


Figure 4. Soil temperature profiles at sites with (a) a 3.0-m-thick sand cover (Yu-4), (b) desertified land with sparse vegetation (Yu-6), (c) a 30-cm-thick sand cover (QH-4), and 1.15-m-thick sand cover (QH-5).

distribution with local heterogeneity in the Honglianghe River basin merely reflects the distribution of permafrost observed elsewhere on the QTP.

The influence of heat and moisture. Xie *et al.*²⁸ suggest that a sand cover or a non-vegetated surface affects the surface radiation and energy budgets of the ground surface as well as the heat and moisture exchange during ground freezing and thawing⁴⁰. For example, the soil temperature under a sand cover with a thickness of less than 20 cm is typically colder than that without a sand cover, but the soil temperature under a sand cover with a thickness greater than 20 cm is typically warmer than that without a sand cover^{30,41,42}. These conclusions are the result of a short-term studies that fails to address the reasons why a sand cover affects the underlying permafrost.

Physical modelling provides some perspective to this problem. According to long-term permafrost temperatures observed in the Beiluhe Basin, the rate of the increase of temperature under alpine meadows is larger than that under alpine steppes and barren lands and is smallest under desert grasslands¹¹. Such variations in permafrost temperatures occur because the thaw of warm permafrost (MAGT at -0.17°C) requires a large amount of latent heat that slowly attenuates the variation of permafrost temperature⁴³.

Moisture content (%)		3	5	7	9	11	13	15
Thermal conductivity (W/(m ³ °C))	Frozen	1.27	1.54	1.86	2.01	2.28	2.38	2.57
	Thawed	1.35	1.5	1.62	1.75	1.88	2.01	2.06

Table 2. Laboratory-measured thermal conductivity of aeolian sand in the Honglianghe River Basin (Dry density: 1650 kg/m³).

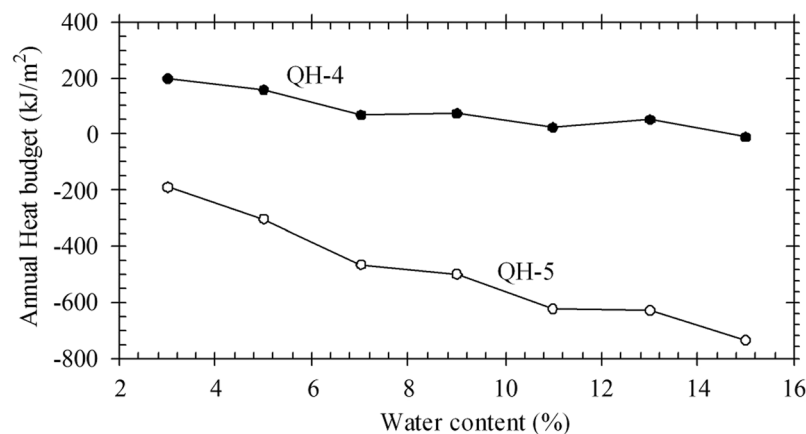


Figure 5. Calculated annual budget of the heat entering the sand layer at depths from 5 cm to 50 cm at sites QH-4 (30 cm sand layer) and QH-5 (115 cm sand layer).

Although details of the heat-moisture transfer that occurs in the surface sand layer are largely unknown, the Fourier Law can be used to approximate the heat fluxes involved using known ground temperatures at a given range of depths:

$$q = -\lambda \frac{T_2 - T_1}{\Delta z} \quad (1)$$

where λ is the thermal conductivity of soil (W·m⁻¹·°C⁻¹), T_1 and T_2 are the temperatures of the lower and upper surfaces of the soil layer (°C), respectively, and Δz is the thickness of the soil layer (m). The thermal conductivity of soil is a function of bulk density, moisture (mainly water or ice) content and temperature gradient⁴⁴. Therefore, the soil moisture content determines the heat fluxes at a given depth. The thermal conductivity of sand in the Honglianghe River Basin, as measured in a laboratory, ranges from 0.85 to 2.75 W/(m°C) in accordance with an increase in the water content from 3% to 15%⁴⁵. The thermal conductivity of dry sand is 10 times less than that of water-saturated sand.

To understand the thermal effect of soil moisture content on heat flux, one can use equation (1) and typical thermal conductivity values (Table 2) to calculate the heat fluxes entering the sand layer at depths from 5 cm to 50 cm. It is assumed that the moisture content of aeolian sand varies from 3% to 15%. By integrating the heat fluxes over a whole year, the annual budget of heat entering the sand layer at depths from 5 cm to 50 cm can be obtained. This is shown in Fig. 5.

It is clear that the annual heat budget of the sand layer progressively decreases with an increase in moisture content (Fig. 5). In other words, dry sand is in a state of extensive absorptive heat over the course of a year; this is a disadvantage to the protection of the underlying permafrost. For example, for site QH-5 (with permafrost), the annual heat budget in the active layer is 734 kJ/m², but in the Chumaerhe Plain, where the climate condition is similar to that of the Honglianghe River region, the annual heat budget in the active layer at a depth of 50 cm to 1.0 m can be up to 12568 kJ/m². It can be concluded, therefore, that a sand layer with high moisture content can better preserve the underlying permafrost only if heat convection is not considered.

Generally, high water content can be a double-edged sword. On the one hand, ice-rich permafrost is difficult to thaw because of latent heat; on the other hand, frequent water movement induces high amounts of heat convection. The latter is many times more effective than heat conduction, radiation, or their combination. In addition, soils with high water content are difficult to freeze because of latent heat. Therefore, discussion must focus upon permafrost that already contains a high ice content. In this situation, what is the role of the sand layer? According to Xie *et al.*, it acts as a thermal diode, having better heat removal properties but being less effective with respect to heat absorption²⁸. In other words, it serves similarly to a coarse block field, as applied successfully to QTR embankments⁴⁶. Peat is another example. Soil moisture is typically low during summer but it becomes water-saturated and ice-rich in autumn and winter, at which time it has a much higher thermal conductivity. This is well documented in the geocryological literature. As a result, peat favours the preservation of marginal permafrost. Unfortunately, the sand layer does not have such unique thermal properties.

A further consideration is that an aeolian sand layer, or a sand dune, has a high infiltration rate and a very low water holding capacity, i.e., rainfall quickly infiltrates. Thus, it is difficult to maintain a high water content within a sand layer in a cold desert environment. For example, *in-situ* drilling in the Honglianghe River Basin showed that the water content within sand layers was always low. At site Yu-4 (see Table 1), the moisture content of the sand layer at depths from 5 cm to 60 cm ranged from 0.1 to 5.2% (average of 2.8%). Similar values at depths from 5 cm to 1 m at site QH-4 ranged from 6.5% to 18.9% (average of 9.0%) and that at site QH-5 ranged from 7.4% to 26.7% (average of 14%). If the effect of local rainfall is removed, the water content within the sand layer becomes less than 10%. It follows that dry sand layers in the Honglianghe River Basin cannot play a role in protecting the underlying permafrost.

Conclusions

Desertification cannot play a role in protecting the underlying permafrost of the Qinghai-Tibet Plateau for the following reasons: (1) Permafrost distribution has a strong spatial heterogeneity. Changes in permafrost temperatures are not simply caused by the ground surface being covered with a sand layer; (2) Soil temperatures measured at nine sites in of the Honglianghe River Basin suggest that permafrost temperatures at sites with varying thicknesses of sand cover can be either colder or warmer than those without a sand cover. Local changes in permafrost temperature cannot be solely determined by the thickness of the sand layer or sand cover; (3) The annual heat budget within a sand layer mainly depends on its moisture content. A high moisture content can better preserve underlying permafrost when heat convection due to rainfall infiltration during the summer is disregarded. However, a sand layer generally cannot maintain a high water content because of enhanced rainfall infiltration.

References

- French, H. M. The Periglacial Environments (3rd ed.) Ch. 5, permafrost, 83 (Wiley Press, 2007).
- Burn, C. R. & Nelson, F. E. Comment on “A projection of severe near-surface permafrost degradation during the 21st century” by David M. Lawrence and Andrew G. Slater. *Geophys. Res. Lett.* **33**, L21503, doi:10.1029/2006GL027077 (2006).
- Cheng, G. D. Influences of local factors on permafrost occurrence and their implications for Qinghai-Xizang Railway design. *Sci China Ser D-Earth Sci* **47**, 704–709, doi:10.1360/02ydo438 (2004).
- Brown, J., Hinkel, K. M. & Nelson, F. E. The Circumpolar Active Layer Monitoring (CALM) Program: Research design and initial results. *Polar Geogr.* **24**, 165–253, doi:10.1080/10889370009377698 (2000).
- Hinkel, K. M. & Nelson, F. E. Spatial and temporal patterns of active layer thickness at Circumpolar Active Layer Monitoring (CALM) sites in northern Alaska, 1975–2000. *J. Geophys. Res.* **108**(D2), 8168, doi:10.1029/2001JD000927 (2003).
- Frauenfeld, O. W., Zhang, T. & Barry, R. G. Interdecadal changes in seasonal freeze and thaw depths in Russia. *J. Geophys. Res.* **109**, D05101–9, doi:10.1029/2003JD004245 (2004).
- Nelson, F. E. (Un) frozen in time. *Science* **299**, 1673–5, doi:10.1126/science.1081111 (2003).
- Camille, P. & Clark, J. S. Long-term perspectives on lagged ecosystem responses to climate change permafrost in boreal peatlands and the grassland/woodland boundary. *Ecosystems* **3**, 534–544, doi:10.1007/s100210000047 (2000).
- Shiklomanov, N. I. *et al.* Decadal variations of active-layer thickness in moisture-controlled landscapes, Barrow, Alaska. *J. Geophys. Res.-Biogeochem* **115**, G00104, doi:10.1029/2009JG001248 (2010).
- Wang, G., Liu, G., Li, C. & Yan, Y. The variability of soil thermal and hydrological dynamics with vegetation cover in a permafrost region. *Agric. For. Meteorol.* **162–163**, 44–47 (2012).
- Wu, Q., Hou, Y., Yun, H. & Liu, Y. Changes in active layer thickness and thermal state of permafrost between 2002–2012 in a variety of alpine ecosystem, Qinghai-Xizang (Tibet) Plateau, China. *Glob. Planet. Chang* **124**, 149–155, doi:10.1016/j.gloplacha.2014.09.002 (2015).
- Cheng, G. D. Problems on zonation of high-altitude permafrost. *Acta Geograph. Sinica* **39**, 185–193 (1984).
- Cheng, G. & Wu, T. Responses of permafrost to climate change and their environmental significance, Qinghai-Tibet Plateau. *J. Geophys. Res.* **112**, F02S03, doi:10.1029/2006JF000631 (2007).
- Ran, Y. *et al.* Distribution of permafrost in China: Overview of existing permafrost maps. *Permafrost. Periglac. Proc.* **23**, 322–333, doi:10.1002/ppp.v23.4 (2012).
- Wu, Q. & Liu, Y. Ground temperature monitors and its recent change in Qinghai-Xizang Plateau. *Cold Reg. Sci. Technol.* **38**, 85–92, doi:10.1016/S0165-232X(03)00064-8 (2004).
- Jin, H. J. *et al.* Change in frozen ground and eco-environmental impacts in the Sources Area of the Yellow River (SAYR) on the northeastern Qinghai-Tibet Plateau, China. *Environ. Res. Lett.* **4**, 045206, doi:10.1088/1748-9326/4/4/045206 (2009).
- Jin, H., Luo, D., Wang, S., Lü, L. & Wu, J. Spatiotemporal variability of permafrost degradation on the Qinghai-Tibet Plateau. *Sci. Cold Arid Reg.* **3**, 281–305 (2011).
- Zhao, L., Wu, Q., Marchenko, S. S. & Sharkhuu, N. Status of permafrost and active layer in Central Asia during the International Polar Year. *Permafrost. Periglac. Proc.* **21**, 198–207, doi:10.1002/ppp.688 (2010).
- Li, R. *et al.* Temporal and spatial variations of the active layer along the Qinghai-Tibet Highway in a permafrost region. *Chin. Sci. Bull.* **57**, 4609–4616, doi:10.1007/s11434-012-5323-8 (2012).
- Wang, B. & French, H. M. Climate controls and high-altitude permafrost, Qinghai-Xizang (Tibet) Plateau, China. *Permafrost. Periglac. Proc.* **5**, 87–100, doi:10.1002/(ISSN)1099-1530 (1994).
- Yang, M. *et al.* Desertification and its relationship with permafrost degradation in Qinghai-Xizang (Tibet) Plateau. *Cold Reg. Sci. Technol.* **39**, 47–53, doi:10.1016/j.coldregions.2004.01.002 (2004).
- Hu, G., Jin, H., Dong, Z., Lu, J. & Yan, C. Driving forces of aeolian desertification in the source region of the Yellow River: 1975–2005. *Environ. Earth Sci* **70**, 3245–3254, doi:10.1007/s12665-013-2389-9 (2013).
- Wang, S., Jin, H., Li, S., Zhao, L. & Guo, D. Permafrost degradation on the Qinghai-Tibet Plateau and its environmental impacts. *Permafrost. Periglac. Proc.* **11**, 43–53, doi:10.1002/(ISSN)1099-1530 (2000).
- Wu, Q., Dong, X., Liu, Y. & Jin, H. Responses of permafrost on the Qinghai-Tibet Plateau, China, to climate change and engineering construction. *Arct. Antarct. Alp. Res.* **39**, 682–687 (2007).
- Jin, H., Yu, Q., Lü, L., Guo, D. & Li, Y. Degradation of permafrost in the Xing’anling Mountains, Northeastern China. *Permafrost. Periglac. Proc.* **18**, 245–258, doi:10.1002/ppp.589 (2007).
- Xie, S. *et al.* Effect of sandy sediments produced by the mechanical control of sand deposition on the thermal regime of underlying permafrost along the Qinghai-Tibet Railway. *Land Degrad. Dev.* **24**, 453–462 (2013).
- Xie, S., Qu, J., Zu, R., Zhang, K. & Han, Q. New discoveries on the effects of desertification on the ground temperature of permafrost and its significance to the Qinghai-Tibet Plateau. *Chin. Sci. Bull.* **57**, 838–842, doi:10.1007/s11434-011-4901-5 (2012).
- Xie, S., Qu, J., Lai, Y., Xu, X. & Pang, Y. Key evidence of the role of desertification in protecting the underlying permafrost in the Qinghai-Tibet Plateau. *Sci. Rep.* **5**, 15152, doi:10.1038/srep15152 (2015).

29. Huang, Y., Guo, D. & Zhao, X. The desertification in the permafrost region of Qinghai-Xizang Plateau and Its influence on environment. *J Glaciol. Geocryol.* **15**, 52–57 (1993).
30. Wang, S. & Xie, Y. Study on the ground temperature of sandy area in the Qinghai-Xizang Plateau. *J. Desert Res.* **18**, 137–142 (1998).
31. Wang, G., Li, Y., Wu, Q. & Wang, Y. Impacts of permafrost changes on alpine ecosystem in Qinghai-Tibet Plateau. *Sci. China Ser. D-Earth Sci.* **49**, 1156–1169, doi:10.1007/s11430-006-1156-0 (2006).
32. Yang, M., Nelson, F. E., Shiklomanov, N. I., Guo, D. & Wan, G. Permafrost degradation and its environmental effects on the Tibetan Plateau: A review of recent research. *Earth-Sci. Rev.* **103**(1–2), 31–44, doi:10.1016/j.earscirev.2010.07.002 (2010).
33. Wu, Q. & Zhang, T. Recent permafrost warming on the Qinghai-Tibetan Plateau. *J. Geophys. Res.* **113**, D13108, doi:10.1029/2007JD009539 (2008).
34. Zhao, L. *et al.* The extent of permafrost in China during the local Last Glacial Maximum (LLGM). *Boreas* **43**, 688–698, doi:10.1111/bor.2014.43.issue-3 (2014).
35. Vandenberghe, J. *et al.* The Last Permafrost Maximum (LPM) map of the Northern Hemisphere: permafrost extent and mean annual air temperatures, 25–17 ka BP. *Boreas* **43**, 652–666, doi:10.1111/bor.2014.43.issue-3 (2014).
36. Xu, X. & Zhu, L. The moisture and heat conditions of insular permafrost at Liangdao He, Xizang. *Professional Papers on Permafrost Studies of Qinghai-Xizang Plateau* 44–48 (Scientific Press, Beijing, 1983).
37. Wu, Q., Zhang, T. & Liu, Y. Permafrost Temperatures and thickness along the Qinghai-Tibetan Highway. *Glob. Planet. Chang.* **72**, 32–38, doi:10.1016/j.gloplacha.2010.03.001 (2010).
38. Niu, F., Zhang, J. & Zhang, Z. Engineering geological characteristics and evaluation of permafrost in Beiluhe Testing Field of Qinghai-Tibetan Railway. *J. Glaciol. Geocryol.* **24**, 264–269 (2002).
39. Wu, Q., Cheng, G. & Ma, W. An analysis on reliability of permafrost roadbed engineering of Qinghai-Tibet Railroad. *Sci. Technol. Review* **23**, 29–31 (2005).
40. Zu, R., He, Z., Zong, Y., Qu, J. & Niu, Q. Review on the influence of sand accumulation on permafrost in the Tibetan Plateau. *J. Desert Res.* **34**, 1208–1214 (2014).
41. Wang, S., Zhao, L. & Li, S. X. Interaction between permafrost and Desertification on the Qinghai-Tibet Plateau. *J. Desert Res.* **22**, 33–39 (2002).
42. Lü, L. Z. *et al.* Dual Influence of local environmental variables on ground temperatures on the interior-Eastern Qinghai-Tibet Plateau (II): sand-layer and surface water bodies. *J. Glaciol. Geocryol.* **30**, 546–555 (2008).
43. Romanovsky, V. E., Smith, S. L. & Christiansen, H. H. Permafrost thermal state in the polar Northern Hemisphere during the International Polar Year 2007–2009: A Synthesis. *Permafr. Periglac. Process.* **21**, 106–116, doi:10.1002/ppp.689 (2010).
44. Xu, X., Wang, J. & Zhang, L. *Frozen soil physics* (ed. Xu, X.) 77–82 (Scientific Press, Beijing, 2001).
45. Chen, L. *et al.* Conductivity of aeolian sand on the Tibetan Plateau based on microstructure. *J Glaciol. Geocryol.* **36**, 1220–1226 (2014).
46. Sheng, Y., Zhang, J., Liu, Y. & Wu, J. Thermal regime in the embankment of Qinghai-Tibetan Highway in permafrost regions. *Cold Reg. Sci. Technol.* **35**, 35–44, doi:10.1016/S0165-232X(02)00026-5 (2002).

Acknowledgements

This study was supported by the Key Research Program of Frontier Sciences, CAS (Grant No. QYZDJ-SSW-DQC011), National Natural Science Foundation of China (Grant No. 41330634), and STS Project of the Chinese Academy of Sciences (Grant No. HHS-TSS-STS-1502). Editing of the manuscript by Professor Hugh French is gratefully acknowledged.

Author Contributions

W.Q.B. and Y.W.B. designed the study and analysed the data, W.Q.B. wrote the manuscript, and J.H.J. reviewed the manuscript. All authors discussed the results and contributed to the manuscript.

Additional Information

Competing Interests: The authors declare that they have no competing interests.

Publisher's note: Springer Nature remains neutral with regard to jurisdictional claims in published maps and institutional affiliations.



Open Access This article is licensed under a Creative Commons Attribution 4.0 International License, which permits use, sharing, adaptation, distribution and reproduction in any medium or format, as long as you give appropriate credit to the original author(s) and the source, provide a link to the Creative Commons license, and indicate if changes were made. The images or other third party material in this article are included in the article's Creative Commons license, unless indicated otherwise in a credit line to the material. If material is not included in the article's Creative Commons license and your intended use is not permitted by statutory regulation or exceeds the permitted use, you will need to obtain permission directly from the copyright holder. To view a copy of this license, visit <http://creativecommons.org/licenses/by/4.0/>.

© The Author(s) 2017